CHEMISTRY
A European Journal

A Journal of
ChemPubSoc Europe

Accepted Article

Title: Novel Synthesis of Anhydrous and Hydroxylated CuF2 Nanoparticles and Their Potential for Lithium Ion Batteries

Authors: Erhard Kemnitz, Thoralf Krahl, Friederike Wnkelmann, Andrea Martin, and Nicola Pinna

This manuscript has been accepted after peer review and appears as an Accepted Article online prior to editing, proofing, and formal publication of the final Version of Record (VoR). This work is currently citable by using the Digital Object Identifier (DOI) given below. The VoR will be published online in Early View as soon as possible and may be different to this Accepted Article as a result of editing. Readers should obtain the VoR from the journal website shown below when it is published to ensure accuracy of information. The authors are responsible for the content of this Accepted Article.

To be cited as: *Chem. Eur. J.* 10.1002/chem.201800207

Link to VoR: http://dx.doi.org/10.1002/chem.201800207

Supported by
ACES

WILEY-VCH

Novel Synthesis of Anhydrous and Hydroxylated CuF_2 Nanoparticles and Their Potential for Lithium Ion Batteries

Thoralf Krahl[1,2], Friederike Marroquin Winkelmann[1], Andréa Martin[1], Nicola Pinna[1], Erhard Kemnitz [1,2]*

[1] Humboldt-Universität zu Berlin, Institut für Chemie, Brook-Taylor-Str. 2, D-12489 Berlin, GERMANY
[2] Nanofluor GmbH, Rudower Chaussee 29, D-12489 Berlin, GERMANY
* tel: +49 30 2093 7555, fax: +49 30 2093 7277, mail: erhard.kemnitz@chemie.hu-berlin.de

Abstract

Anhydrous nanoscopic CuF_2 is synthesized from alkoxides $Cu(OR)_2$ (R = Me, ^{t}Bu) by their reaction either in pure liquid HF at -70°C, or under solvothermal conditions at 150°C using excess HF and THF as solvent. Depending on the synthesis method, nanoparticles of sizes between 10 and 100 nm are obtained. The compound is highly hygroscopic and forms different hydrolysis products under moist air, namely $CuF_2{\cdot}2H_2O$, $Cu_2(OH)F_3$ and Cu(OH)F, of which only the latter is stable at room temperature. CuF_2 exhibits an electrochemical plateau at a potential of ~2.7 V when cycled versus Li in half cell Li-ion batteries, which is attributed to a non-reversible conversion mechanism. The cell capacity in the first cycle depends on the particle size, being 468 mAh g^{-1} for ≈8 nm crystallite diameter, and 353 mAh g^{-1} for ≈12 nm crystallite diameter, referred to CuF_2. However, such a high capacity cannot be sustained for several cycles and the capacity rapidly fades out. The cell voltage decreases to ~2.0 V for $CuF_2{\cdot}2H_2O$, $Cu_2(OH)F_3$ and Cu(OH)F. Because all the compounds studied in this work show irreversible conversion reactions we conclude that copper-based fluorides are unsuitable for Li-ion battery applications.

1 Introduction

The search for new materials for Li-ion batteries has become essential during the last years, because the compounds used nowadays as cathodes for commercial applications have reached their limit of performance. The chemistry involved in these electrochemical processes is based on the intercalation reaction of a structure able to intercalate Li^+ ions in a reversible way. The commonly used compounds such as $LiFePO_4$ or $LiCoO_2$, with practical capacities comprised in the range of 120-180 mAh g^{-1}, can theoretically host no more than 1 Li per unit formula, hence limiting the theoretical capacity of these materials. One of the strategies that the scientific community has pursued is based on materials storing lithium ions via conversion reactions enabling more than one lithium to react per formula unit. This reaction allows reaching a much higher capacity than those obtained with intercalation materials. This class of compounds comprises mostly metal oxides and fluorides.[1] The conversion reaction follows the scheme below:

$$M_aX_b + bn\ Li \rightleftarrows a\ M + b\ Li_nX \quad (1)$$

M = transition metal, n = stoichiometry of Li against X, X = anion (O, F)

Among these compounds, only the metal fluorides have redox potentials in the region of 2.6-3.5 V being high enough to be used as cathode materials in Li-ion batteries. These high potentials are due to the high electronegative character of the metal fluorine bond, and hence, due to the high free energy of formation of LiF. The most studied new materials for application in Li-ion batteries are the fluorides of Fe, Co, Ni and Cu (Table 1). In praxis, all these transition metal fluorides display operating potentials lower than theoretically

Accepted Manuscript

This article is protected by copyright. All rights reserved.

predicted. This is caused by the very low conductivity of this class of compounds arising from their high ionic character, and hence, the slow kinetics of the conversion reaction.

Table 1. Theoretical potential and capacity of selected transition metal fluorides.[1b]

Compound	Theoretical potential (V) [a]	Theoretical capacity (mAh g^{-1}) [b]	Electronic conductivity
FeF_2	2.66	571	none
FeF_3	2.74	712	none
CoF_2	2.85	553	poor
NiF_2	2.96	554	poor
CuF_2	3.55	528	none

[a] MF_n/M vs. Li/LiF, [b] $C_{th} = nF/M_w$

Among these metal fluorides, the copper(II) fluoride CuF_2 presents the highest theoretical potential of 3.55 V and a theoretical capacity of 528 mAh g^{-1}. These properties make it a very interesting electrode material for application in Li-ion batteries.[2]

However, in the literature, very poor cyclabilities have been reported, which may be due to volume changes during the conversion reaction or dissolution of the active material along the cycles.[3] Typically adopted strategies to overcome the poor performance of transition metal fluorides, which is mainly attributed to their insulating character, are the reduction of the particle size and their combination with conductive agents.[4] It can be stated that in general the application of such materials in nanoparticular form is favored over materials consisting of large crystallites.

It has also been shown recently that protecting the metal fluorides from the dissolution through coating or the use of suitable additive in the electrolyte could improve the cycling stability.[5]

The synthesis of anhydrous CuF_2 is a challenging task. In aqueous chemistry, either the dihydrate $CuF_2{\cdot}2H_2O$ or various hydroxide fluorides are obtained. Dehydration of $CuF_2{\cdot}2H_2O$ does not lead to CuF_2, but rather to different hydrolyzed products like Cu(OH)F, $Cu_2(OH)F_3$, $Cu_3(OH)_2F_4$ or even CuO depending on the reaction conditions.[6]

Anhydrous CuF_2 is a highly hygroscopic white solid crystallizing in a Jahn-Teller distorted rutile structure.[7] There are only few synthesis methods known. CuF_2 can be synthesized as bulk material by the reaction of Cu metal with F_2 or a mixture Cl_2/F_2; or by reaction of copper halides with F_2.[8] CuO or $CuF_2{\cdot}2H_2O$ can be reacted with a stream of dry gaseous HF at high temperatures (>300°C) to form CuF_2.[9] In a different approach, first the complex fluorides NH_4CuF_3 and $(NH_4)_2CuF_4$ are formed by reaction of appropriate precursors ($CuCl_2$, $CuBr_2$ or $CuF_2{\cdot}2H_2O$) with NH_4F or NH_4HF_2 either in a solvent or as solid-solid reaction, followed by thermal decomposition.[10]

The well-established thermal decomposition of metal trifluoroacetates into fluorides, especially for $Ae(CF_3COO)_2$ (Ae = Ca, Sr, Ba),[11] fails in the case of $Cu(CF_3COO)_2$, ending up with a mixture of CuO and Cu_2O.[12]

Accepted Manuscript

This article is protected by copyright. All rights reserved.

Most of these publications are quite old and are lacking some of the modern analysis methods. Moreover, these methods are based on high temperature syntheses, resulting in highly crystalline bulk material rather than nanoparticles.

The aim of this publication is to explore new approaches for the direct synthesis of nanoscale CuF_2 particles based on soft chemistry, and also to verify some of the previously reported methods.

A promising candidate for the synthesis of copper fluoride is the fluorolytic sol-gel synthesis, which was successfully applied to many different binary metal fluorides in the last decade ($M^{I}F$, $M^{II}F_2$, $M^{III}F_3$; M^{I} = Li, M^{II} = Mg, Ca, Sr, Ba, Zn; M^{III} = Al, Y, Yb).[13] However, the synthesis of copper(II) compounds was yet not reported. An appropriate metal precursor is reacted with anhydrous HF dissolved in a non-aqueous solvent (mostly alcohols or ethers), resulting in sols of nanoscale metal fluorides:

$$MX_n + 2\ aHF_{solv} \xrightarrow{solv} nano\text{-}MF_n + 2\ HX \qquad (2)$$

(M = metal; X = halide, alkoxide, carboxylate, etc.; solv = alcohol, ether; aHF = anhydrous HF)

In general, the most appropriate precursors are metal alkoxides, carboxylates or halides. The optimal precursor depends on the metal ion, solvent and reaction conditions.

In this work, the fluorolytic sol-gel synthesis of anhydrous CuF_2 is reported, as well the use of CuF_2 as positive electrode in Li-ion batteries. Cyclic voltammetry and galavanostatic cycling are applied to investigate the electrochemical behavior. For a deeper understanding of the lithiation mechanisms, oxygen-containing fluorinated copper compounds $CuF_2{\cdot}2H_2O$, $Cu(OH)F$ and $Cu_2(OH)F_3$ were synthesized and their electrochemical properties compared.

2 Results and Discussion

2.1 Synthesis of anhydrous CuF_2 and related compounds

2.1.1 Thermodynamics of the formation of CuF_2

According to the hard and soft (Lewis) acids and bases (HSAB) concept, the copper(II) ion is comparatively soft. This fact is a significant difference to the ions of Mg, Ca, Sr, Ba and Zn, for which the fluorolytic sol gel synthesis of nanoscale binary fluorides is well known.[13] The affinity of Cu^{2+} towards F^- is low, but it is much higher towards the heavier halogens Cl^- and Br^-. To illustrate the different reactivity of the different divalent metal ions, reaction enthalpies for the fluorination of anhydrous divalent metal chlorides and acetates are given in Table 2.

Accepted Manuscript

This article is protected by copyright. All rights reserved.

Table 2. Standard reaction enthalpy of divalent metal precursors with hydrogen fluoride (in kJ mol^{-1}). $OAc^- = CH_3COO^-$ (acetate). Thermodynamic data is taken from ref. [14]

M	$MCl_{2(s)} + 2\ HF_{(g)} \rightarrow MF_{2(s)} + 2\ HCl_{(g)}$	$M(OAc)_{2(s)} + 2\ HF_{(g)} \rightarrow MF_{2(s)} + 2\ HOAc_{(g)}$	$M(OH)_{2(s)} + 2\ HF_{(g)} \rightarrow MF_{2(s)} + 2\ H_2O_{(g)}$
Mg	-119.6		-138.3
Ca	-73.5	-69.3	-181.8
Sr	-27.0 [a]	-48.4	-195.8
Ba	+3.5 [a]	-50.5	-209.4
Zn	+11.1	-5.3	-61.1 [b]
Cu	+39.5	+34.9	-27.7 [b]

[a] These chlorides form chlorofluorides upon reaction with HF: $MCl_{2(s)} + HF_{(g)} \rightarrow MClF_{(s)} + HCl_{(g)}$: ΔH = -36.9 (Sr); -25.6 (Ba) kJ mol^{-1}. [b] These fluorides are hygroscopic and form hydrates.

Thus, the low affinity of Cu^{2+} towards fluoride must be compensated by a very basic counter anion X^- having a high reactivity towards HF (cf. Table 2, right column). $Cu(OH)_2$ is not suitable for that purpose, because CuF_2 is highly hygroscopic and reacts with the water formed during the fluorination. Instead, most suitable for this purpose are copper(II) alkoxides $Cu(OR)_2$. The methoxide and the *tert*-butoxide were synthesized (cf. experimental section) and were used in the fluorolytic sol-gel process. $Cu(OMe)_2$ is the base compound, which can be directly synthesized from $CuCl_2$ and LiOMe. Cu^{2+} is a strong oxidizing agent, and therefore, all copper(II) alkoxides of primary and secondary alcohols are decomposed easily at elevated temperatures into Cu_2O or Cu and aldehydes or ketones. Tertiary alcohols are more stable towards oxidants, and hence, reactions with $Cu(O\mathit{t}Bu)_2$ in either *tert*-butanol or tetrahydrofuran can also be performed at higher temperatures. Other copper alkoxides of primary and secondary alcohols can be synthesized *in situ* by refluxing $Cu(OMe)_2$ with an excess of the corresponding alcohol and simultaneous evaporation of methanol.

2.1.2 Synthesis of anhydrous CuF_2

The simple reaction of stoichiometric amounts of solvated HF with $Cu(OR)_2$ in alcohols or THF does not lead to the formation of CuF_2. Using a large excess of HF (10-20 fold), indeed, CuF_2 may be formed in small amounts (cf. next section), but the product is not pure. For a complete conversion of the alkoxide, more drastic reaction conditions are necessary: (i) Higher temperature and pressure using solvated HF under solvothermal conditions, or (ii) performing the reaction in liquid unsolvated anhydrous HF.

$$Cu(OR)_2 + 2\ HF \rightarrow CuF_2 + 2\ ROH \quad (R = Me, \mathit{t}Bu) \qquad (3)$$

$Cu(OR)_2$ (R = Me, *t*Bu) reacts with a 10-fold excess of HF in THF solution in a Teflon-lined autoclave under argon atmosphere at 150°C and 8 bar within 2 hours. CuF_2 is obtained as white precipitate (CuF_2-1 from $Cu(OMe)_2$ and CuF_2-2 from $Cu(O\mathit{t}Bu)_2$ in Table 3). The supernatant THF has a brownish appearance. Obviously, a part of copper(II) was reduced (most probably to Cu_2O or Cu), but the amount is very small (far below 1%). The product can be simply decanted or filtered and subsequently washed with THF at -20°C. Unfortunately, CuF_2 seems to have a certain solubility in THF even at -20°C, therefore the synthesis yield is comparatively low (<50%).

Accepted Manuscript

This article is protected by copyright. All rights reserved.

The reaction of $Cu(OR)_2$ (R = Me, *t*Bu) with pure liquid anhydrous HF at -70°C also leads to white CuF_2 within a few seconds upon stirring of the reaction mixture. After allowing the reaction vessel to heat up to room temperature, excess HF evaporates. Adsorbed HF and the alcohol formed during the reaction can be pumped off in vacuum. A further cleaning process is not necessary, pure white CuF_2 is obtained directly (CuF_2-3 from $Cu(OMe)_2$ and CuF_2-4 $Cu(O$*t*$Bu)_2$ in Table 3). The yields are generally higher than in the autoclave reaction (70-80%).

Analysis data of the products is given in Table 3, for XRD cf. Figure 1. The fluorine-to-copper-ratio is nearly 2 in all products. The samples contain about 6-12% of organic residue, which is typical for nanoparticles synthesized form organic precursors. The organic residue further stabilizes the surface of the particles.[13] X-ray powder diffractograms of 3 out of these 4 synthesized CuF_2 samples show exclusively reflections of CuF_2 (Figure 1), which are broadened due to the small crystallite sizes. According to Scherrer's equation, the crystallite sizes range from 14 to 23 nm. Only CuF_2-3, i.e. from the reaction of $Cu(OMe)_2$ with liquid HF at -70°C, is not pure in the XRD, but shows some additional unknown reflections between 10 and 20°.

Table 3. Properties of different samples of CuF_2. Calcd (%): Cu 62.58, F 37.42.

Name	Reactant	*Reaction method*	Cu (%)	F (%)	C (%)	H (%)	res (%) [a]	n_F/n_{Cu} [b]	XRD [c]
CuF_2-1	$Cu(OMe)_2$	*solvothermal*	58.80	34.50	0.37	2.76	6.70	1.96	CuF_2 only $L \approx 23$ nm
CuF_2-2	$Cu(O$*t*$Bu)_2$	*solvothermal*	58.63	34.40	1.43	0.53	6.97	1.96	CuF_2 only $L \approx 20$ nm
CuF_2-3	$Cu(OMe)_2$	*liquid HF*	56.32	33.30	2.77	1.48	10.38	1.98	*nearly amorphous* + unk. refl.
CuF_2-4	$Cu(O$*t*$Bu)_2$	*liquid HF*	56.10	32.20	4.25	3.75	11.70	1.92	CuF_2 only $L \approx 14$ nm

[a] residue = 100–Cu–F. [b] molar ratio of F and Cu in the product. [c] L = size of the coherent scattering region according to Scherrer's equation

Accepted Manuscript

This article is protected by copyright. All rights reserved.

10.1002/chem.201800207

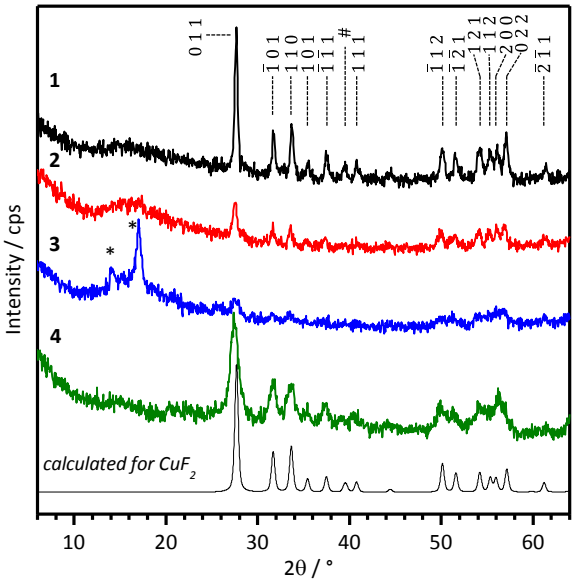

Figure 1. XRD of different samples of CuF_2 (cf. Table 3) and expected diffractogram calculated from single crystal data. Miller indices for the observed reflections are given above. Note that not all expected reflections are observed due to their broadness. (#) Overlap of 0 1 2 and 0 2 1. (*) Unknown phase.

TEM images of CuF_2 synthesized under solvothermal conditions show large aggregates of a size of several hundred nanometers (Figure 2A). The size and shape of the primary particles cannot be clearly determined, at least some particles are smaller than 50 nm. On the other hand, the particles of CuF_2 synthesized in liquid HF are smaller and less aggregated. The primary particles are spherical, their size is around 10 nm, and the size of the aggregates around 30 nm (Figure 2B). Thus, the reaction at -70°C in liquid anhydrous HF leads to significantly smaller CuF_2 particles than the solvothermal synthesis.

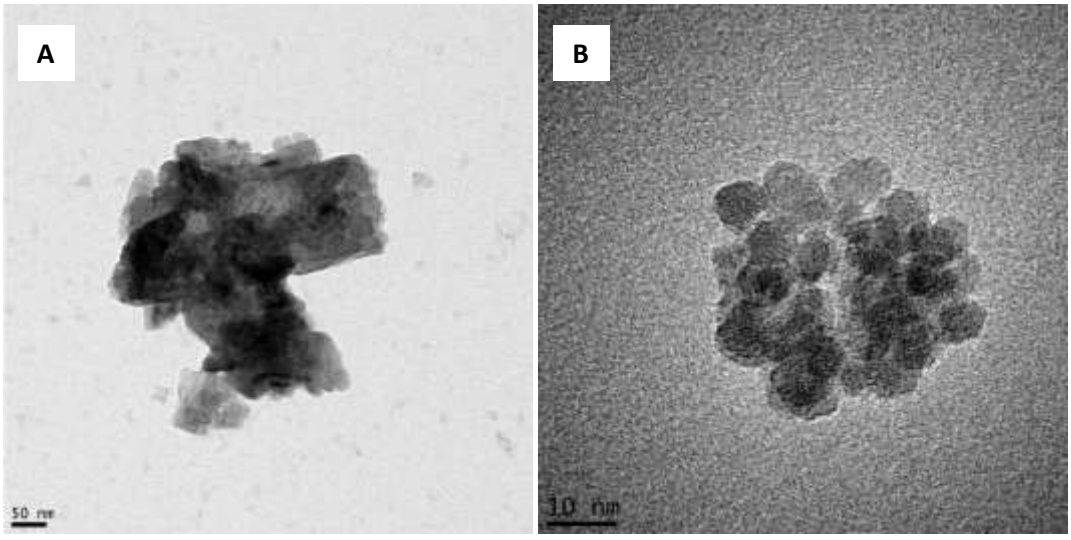

Figure 2. TEM images of (A) CuF_2-1 from solvothermal synthesis (scale 50 nm) and (B) CuF_2-4 from reaction in liquid HF (scale 10 nm).

Accepted Manuscript

This article is protected by copyright. All rights reserved.

2.1.3 Synthesis of Cu(OR)F, $CuF_2{\cdot}2H_2O$, $Cu_2(OH)F_3$ and Cu(OH)F

Cu(OR)F. As already mentioned in the previous section, the reaction of copper(II) alkoxides with solvated HF at ambient temperature and pressure under argon atmosphere does not lead to the formation of CuF_2. Instead, a new class of compounds Cu(OR)F is formed:

$$Cu(OR)_2 + HF_{solv} \rightarrow Cu(OR)F + ROH \quad (4)$$

These compounds are not subject of this investigation. Details and further information can be found in the supporting information (FTIR: Figure S1, XRD: Figure S2).

$CuF_2{\cdot}2H_2O$. Synthesis of phase pure $CuF_2{\cdot}2H_2O$ from aqueous solutions is a challenging task, because it requires accurate control of reaction conditions; otherwise mixtures of different compounds are obtained. $CuF_2{\cdot}2H_2O$ readily undergoes hydrolysis reactions, resulting in different hydroxide fluorides. The main side product is always Cu(OH)F, and to a lesser extend $Cu_2(OH)F_3$, but even CuO was observed.

Therefore, a new synthesis from non-aqueous solvents was developed in order to reduce the number of side reactions. The reaction of $CuCO_3{\cdot}Cu(OH)_2$ in ethanol with an excess of ethanolic HF (molar ratio HF:Cu = 3:1) in an open PFA flask leads nearly quantitatively to the desired product within one hour under generation of CO_2:

$$CuCO_3{\cdot}Cu(OH)_{2(s)} + 4\ HF + H_2O \rightarrow 2\ CuF_2{\cdot}2H_2O\downarrow + CO_2\uparrow \quad \text{(in ethanol)} \quad (5)$$

One equivalent of water is obviously absorbed from the surrounding air. The light blue precipitate can be filtered off and dried in vacuum. This reaction in ethanol delivers a nanocrystalline aggregated product. These aggregates have a size of ≈100-300 nm and consist of primary particles with a size far below 50 nm (Figure 3A). When the product is stored under argon, it is stable for long time (at least 6 months). At ambient air, it decomposes within a couple of days into Cu(OH)F (Figure 4).

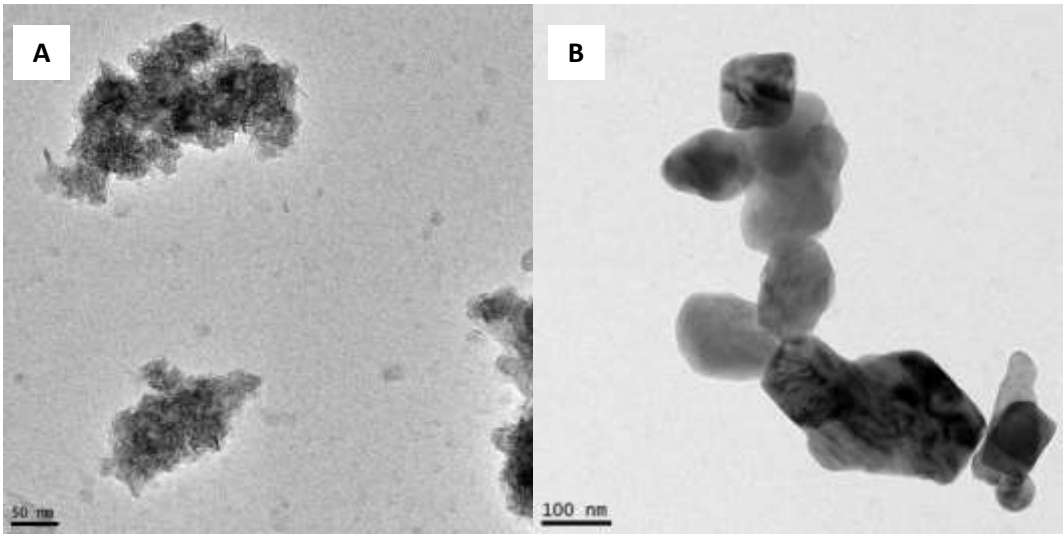

Figure 3. TEM images of (A) $CuF_2{\cdot}2H_2O$ from reaction in methanol (scale 50 nm) and (B) Cu(OH)F from reaction in boiling water (scale 100 nm).

Accepted Manuscript

This article is protected by copyright. All rights reserved.

Upon heating under inert gas, the proposed dehydration mechanism of $CuF_2{\cdot}2H_2O$ is different:[6, 15]

$$2\,CuF_2\cdot 2H_2O \xrightarrow[\substack{-HF\\-3H_2O\\\Delta m_1=26.92\%}]{130\text{-}180^\circ C} Cu_2(OH)F_3 \xrightarrow[\Delta m_2=7.27\%]{\approx 420^\circ C,\ -HF} CuO + CuF_2 \qquad (6)$$

The published temperatures of the two mass loss steps differ from each other. Our own thermal analysis of $CuF_2{\cdot}2H_2O$ in an argon stream revealed a temperature of 176°C for the first step and 391°C for the second step applying a heating rate of 10 K min^{-1} (cf. SI Figure S3). At a lower heating rate of 1 K min^{-1}, the first decomposition step is shifted to 156°C (cf. SI Figure S4).

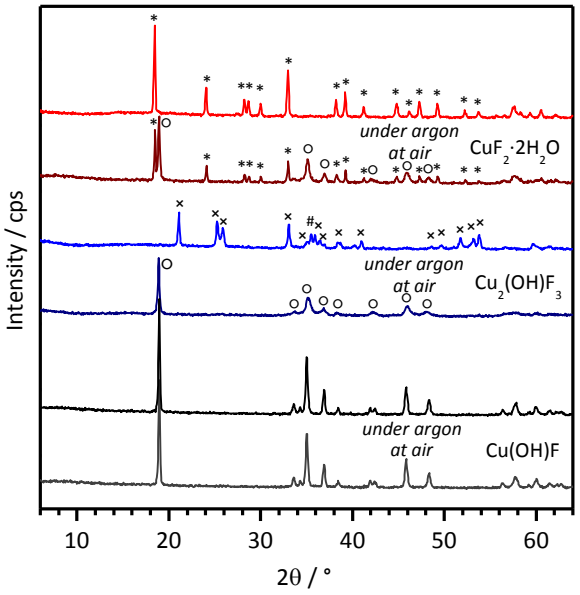

Figure 4. XRD of hydrated copper(II) fluorides and hydroxide fluorides as prepared under argon and after exposure to air for 5 days. (#) One unknown reflection, probably CuO.

$Cu_2(OH)F_3$. $Cu_2(OH)F_3$ is formed as a side product during reactions in aqueous solutions containing Cu^{2+} and HF, but a synthesis of the pure product is not possible in this way. Thermal dehydration of $CuF_2{\cdot}2H_2O$ upon heating in inert atmosphere theoretically leads to the desired compound (eq. 6), but carried out as a bulk reaction, only product mixtures were obtained and not a phase pure substance. Thus, the conditions of the thermal decomposition need to be finely adjusted.

Nearly phase pure $Cu_2(OH)F_3$ is obtained upon thermal decomposition of $CuF_2{\cdot}2H_2O$ under self-generated atmosphere (instead of applying vacuum or an inert gas stream) at 160°C:

$$2\,CuF_2{\cdot}2H_2O \rightarrow Cu_2(OH)F_3 + 3\,H_2O\uparrow + HF\uparrow \qquad (7)$$

The compound is of a very light blueish color. It is highly moisture sensitive and has to be stored and handled under argon. Although the crystal structure of $Cu_2(OH)F_3$ was not solved,

Accepted Manuscript

This article is protected by copyright. All rights reserved.

its published XRD pattern is in good agreement with what we report here.[6] At moist air, it hydrolyzes within a few minutes into Cu(OH)F (Figure 4).

Cu(OH)F. Cu(OH)F seems to be a comparatively stable compound, when water and fluoride are present in the reaction system. There are many ways for its synthesis. At ambient air, the compounds CuF_2, $CuF_2{\cdot}2H_2O$, $Cu_2(OH)F_3$ and Cu(OR)F undergo hydrolysis and are finally transformed into Cu(OH)F. Under these conditions, Cu(OH)F seems to be a stable thermodynamic minimum.

Crystallographic pure Cu(OH)F in larger amounts can be easily synthesized according to Berzelius by boiling $CuF_2{\cdot}2H_2O$ for 5 hours in water in an open plastic beaker:[16]

$$CuF_2{\cdot}2H_2O \rightarrow Cu(OH)F + H_2O\uparrow + HF\uparrow \quad (8)$$

The so-obtained product consists of aggregated particles, the size of the aggregates is several hundred nanometers (Figure 3B). The size of the primary particles is around 100 nm. This is in accordance with the narrow reflections in XRD (Figure 4). The product is stable at moist air for at least several weeks, most probably even months (Figure 4).

2.1.4 Summary of synthesis

An overview about the preparative reactions leading to CuF_2 and its hydrolysis products is given in Figure 5.

The most suitable reactants towards CuF_2, and especially *nano*-CuF_2, are copper(II) alkoxides $Cu(OR)_2$. The reaction of $Cu(OMe)_2$ with HF would be the easiest way towards CuF_2, but this reaction requires harsh conditions. At elevated temperature and pressure, only one methoxide group is fluorinated resulting in the formation of Cu(OMe)F. This compound is very stable, as long as water is excluded. Even the reaction of $Cu(OMe)_2$ with liquid anhydrous HF does not lead to pure CuF_2. Contrary to this, $Cu(O\mathit{t}Bu)_2$ is much more reactive. It reacts with liquid HF at –70°C to spherical CuF_2 nanoparticles below 10 nm in diameter.

Accepted Manuscript

This article is protected by copyright. All rights reserved.

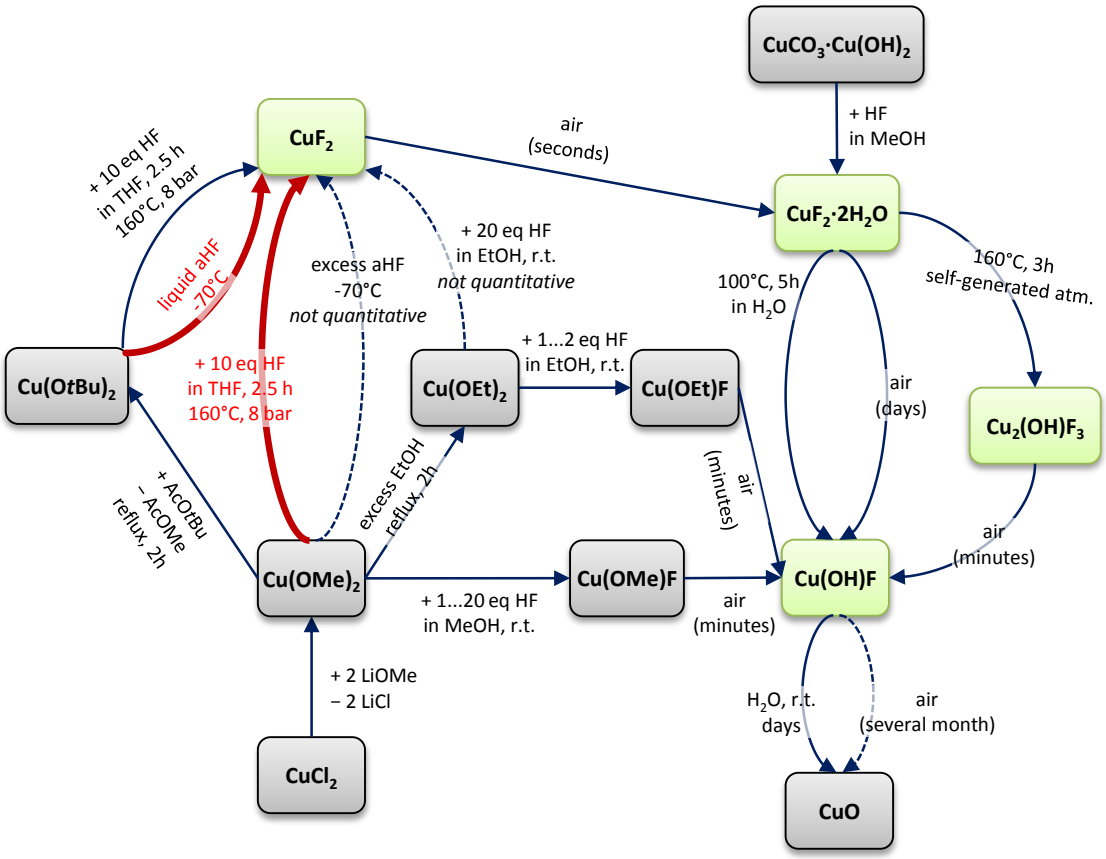

Figure 5. Overview about the synthesis reactions in the CuF_2 system. Thick red arrows: most suitable reactions towards CuF_2. Dashed arrows: product mixtures. Green boxes: compounds used for electrochemical investigations. aHF = anhydrous HF, Me = methyl, Et = ethyl, *t*Bu = *tert*-butyl, AcOMe = methyl acetate, AcO*t*Bu = *tert*-butyl acetate.

In solution, complete fluorination of $Cu(OMe)_2$ or $Cu(OtBu)_2$ to CuF_2 is achieved under solvothermal conditions in THF at 150°C and 8 bar resulting in a nanocrystalline products forming aggregated particles. In this case, the reaction with $Cu(OMe)_2$ is more convenient, because the synthesis of $Cu(OtBu)_2$ requires an additional reaction step.

Thus, the two most suitable synthesis reactions for CuF_2 are:

1. The reaction of $Cu(OMe)_2$ with excess HF in THF at 150°C for 3 h, resulting in nanocrystalline aggregated material.
2. The reaction of $Cu(OtBu)_2$ with excess of pure unsolvated HF at –70°C for 30 min, resulting in slightly agglomerated particles with diameters below 10 nm.

Nearly all compounds containing Cu^{II} and fluoride are moisture sensitive. Even the hydrate $CuF_2{\cdot}2H_2O$ is not stable in air. The only notable exception is Cu(OH)F, which is formed upon exposure to air from CuF_2, $CuF_2{\cdot}2H_2O$, $Cu_2(OH)F_3$ and Cu(OR)F (R = Me, Et).

2.2 Electrochemical properties

2.2.1 Electrochemistry of anhydrous CuF_2

As already mentioned, metal fluorides intrinsically show very low electric conductivity and their integration in electrode materials is difficult. However, their conductivity can be

Accepted Manuscript

This article is protected by copyright. All rights reserved.

increased by combining nanoscale materials with conductive additives. For example, ball milling with carbon black increases the conductivity, enables homogeneous dispersion of the two components, and therefore, lowers the insulating character of the active material.[4b] Upon ball milling of CuF_2 with carbon black, diffraction peaks coming from metallic copper are present (cf. SI Figure S5A). This creation of metallic copper may be due to the reaction between the CuF_2 and the carbon black induced by the energy impact of the mill:

$$CuF_2 + x\,C \rightarrow (1-{}^{x}/_{2})\,CuF_2 + {}^{x}/_{2}\,Cu + CF_x \qquad (9)$$

XRD measurements on the first peaks of CuF_2, after the ball-milling process, point to a decrease of the crystallite sizes for the both compounds, nevertheless the compound CuF_2-4 still exhibits a smaller crystallite size than CuF_2-1 (cf. SI Figure S5B).

Two different samples of CuF_2, synthesized under solvothermal conditions or in liquid HF (cf. Table 3), respectively, were evaluated by cyclic voltammetry and galvanostatic charge/discharge cycling. Figure 6 shows cyclic voltammetry of the small CuF_2-4 particles within two different potential windows.

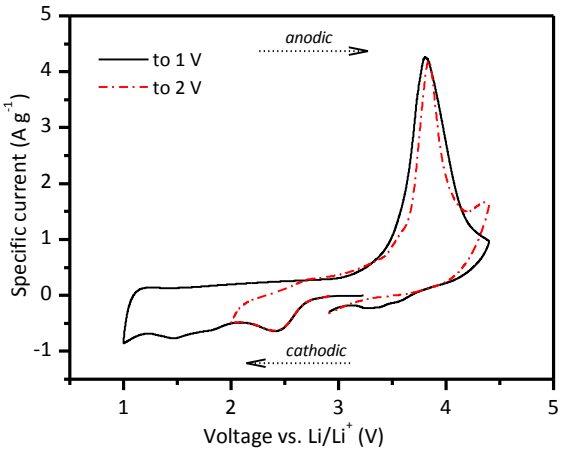

Figure 6. Cyclic voltammetry of CuF_2-4/CB (cf. Table 3) between 1 and 4.5 V and 2 and 4.5 V. Sweeping rate is 1 mV s^{-1}. CB: carbon black.

On the cathodic sweep down to 2 V, a broad peak can be seen starting from ~2.7 V, having its maximum at ~2.5 V. This broad peak can be assigned to the reduction of the fluoride material to metallic copper and lithium fluoride. Extending the cathodic sweep to 1 V, an additional broad peak can be seen at 1.5 V and another one after 1 V. As no reaction is expected at such low potentials, we can assume that these two peaks can be assigned to side reactions probably with the electrolyte.

On the anodic sweep, no obvious peak is present before ~3.2 V. At this region, a large oxidation peak is observed, which is assigned to the dissolution of the metallic copper into the electrolyte (instead of reconversion to CuF_2) during the cathodic sweep. To validate this assumption, a copper plate has been used as cathode for linear sweep potential, which should simulate the metallic copper produced during the reduction of the copper(II) fluoride. As expected, a similar signal can be seen in the potential range of 3.5-3.7 V (cf. SI Figure S6). Furthermore, we can well assign the peak at 2.5 V during the cathodic sweep being the only

Accepted Manuscript

This article is protected by copyright. All rights reserved.

reduction of the CuF_2, because for the cyclic voltammetry the current produced on the anodic sweep during the dissolution of the metallic copper is similar between the potential window 2-4.5 V and 1-4.5 V.

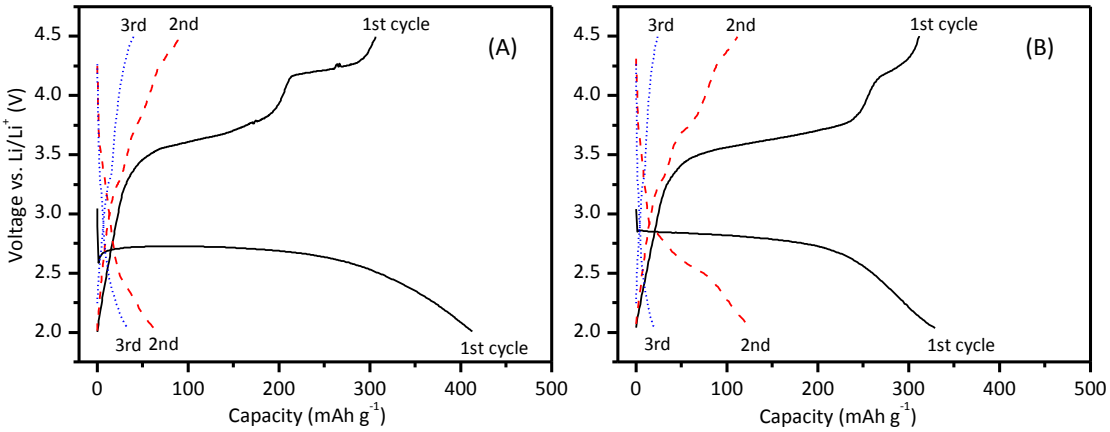

Figure 7. Galvanostatic charge/discharge profiles at 0.1C rate of (A) CuF_2-4/CB (small particles, synthesis in liquid HF) and (B) CuF_2-1/CB (big particles, solvothermal synthesis), Cf. Table 3 and Figure 2 for details. CB: carbon black.

Figure 7 shows the three first discharge/charge profiles of two different samples of CuF_2 cycled at 0.1C. The main difference between these two compounds is the size of the crystallites, which after ball milling is roughly 50% larger larger for CuF_2-1 synthesized under solvothermal conditions (cf. SI Figure 5B). For conversion materials in Li-ion batteries a smaller particle size is generally traduced by an easier diffusion of the electrons and ions within the electroactive material. This would provide faster kinetics of reaction, better reversibility and therefore better performances. It is thought that the reaction path length within this kind of material is around 10 nm.[17] Sizing the particles around this diameter should minimize, and hopefully overcome the conductivity problems. It will also promote the dissolution of metallic copper produced during the conversion reaction, because a larger surface will be exposed to the electrolyte. The samples of CuF_2 show a flat plateau located around 2.7 V, which can be ascribed to the reduction of the CuF_2 to metallic copper and lithium fluoride (cf. CV experiments). For further confirmation, ex-situ X-ray diffraction has been carried out on the electrode material at the end of the discharge (cf. SI Figure S5a). Clear broad signals of lithium fluoride can be observed.

The difference of morphology between the two CuF_2 samples will bring slightly different profiles of discharge. The smaller particles (Figure 7A) present a higher capacity release, namely 413 mAh g^{-1}, the larger particles (Figure 7B) a capacity of 329 mAh g^{-1}, which represents 78% and 62% of the theoretical capacity, respectively, including the organic residue (cf. Table 3). This assumption is confirmed by cycling the composite materials at a higher rate; when the first discharge is operated at 1C, the loss in capacity is smaller for the compound with smaller crystallites (cf. SI Figure S7). It confirms the better performance for smaller particles. The following charges show for both compounds a big plateau around 3.5 V, which can be ascribed to the dissolution of the metallic copper according to the CV experiment (Figure 6). A second plateau around 4.2 V is caused by another side reaction. This

Accepted Manuscript

This article is protected by copyright. All rights reserved.

plateau at high potential could be due to the decomposition of the electrolyte due to the catalytic power of metal fluorides as it has been already observed in the literature.[18] Almost no capacity is released during the second discharge of the CuF_2-4 material, which could be due to the total dissolution of the converted metallic copper. It shows that none of the converted material has been reconverted back during the charge process. The compound CuF_2-1 shows a very small capacity during the second discharge process, which could be due to the incomplete conversion of the nanoparticles during the first discharge. During the third discharge almost no capacity is observed.

Table 4. Electrochemical properties of CuF_2, $Cu(OH)_2$ and related compounds. Thermodynamic data is taken from ref.[14] Measured capacity is for the active material only including the organic residue, but not the carbon black.

Compound	Theoretical potential (V) [a]	Theoretical capacity (mAh g^{-1}) [b]	Crystal structure	Measured potential (V)	Measured capacity at 0.1C rate, 1st cycle (mAh g^{-1})	Measured capacity at 0.1C rate, 10th cycle (mAh g^{-1})
CuF_2	3.55	528	distorted rutile [7]	~2.5	1: 329 (353) [c] 4: 413 (468) [c]	*none*
$CuF_2{\cdot}2H_2O$	3.46	390	chain structure [19]	~2.0	565	77
$Cu_2(OH)F_3$	≈3.2 [d]	533	*unknown*	~2.0	504	72
$Cu(OH)F$	≈3.0 [d]	538	layered structure [20]	~2.0	585	37
$Cu(OH)_2$	2.62	549	layered structure [21]			

[a] vs. Li/(LiF,LiOH). [b] $C_{th} = nF/M_w$. [c] 1: 100 nm, 93.3% CuF_2; 4: 10 nm particle size, 88.3% CuF_2 (cf. Table 3). Values in brackets are corrected for the organic residue and refer to pure CuF_2. [d] estimated from CuF_2 and $Cu(OH)_2$ using an arbitrary correction of -0.1 V for the unknown enthalpy of formation of $Cu(OH)_xF_{2-x}$.

2.2.2 Electrochemistry of $CuF_2{\cdot}2H_2O$, $Cu_2(OH)F_3$ and $Cu(OH)F$

When a certain amount of oxygen replaces fluorine ions in metal fluorides their conductivity is improved. This should lower the average ionic character of the compound and decrease the polarity of the metal fluorine bond. The exact role of hydroxide groups in metal fluorides has not been yet fully discussed, but it is known to play an important role. This has been shown especially for the iron fluoride system, where the total fluorination of the compound is quite hard following a soft-chemistry approach. The introduction of water into the structure facilitates the diffusion of the lithium ions within the framework by creating channels, in which the ions can diffuse more easily, and hence, improving the performance of the material.[22] The expected theoretical potentials and capacities of the relevant copper(II) fluoride hydrate or hydroxide materials are summarized in Table 4. It is expected, that the cell potential of $Cu(OH)_xF_{2-x}$ is lower than that of anhydrous CuF_2. This effect is mainly caused by the lower enthalpy of formation of LiOH compared to LiF.

Accepted Manuscript

This article is protected by copyright. All rights reserved.

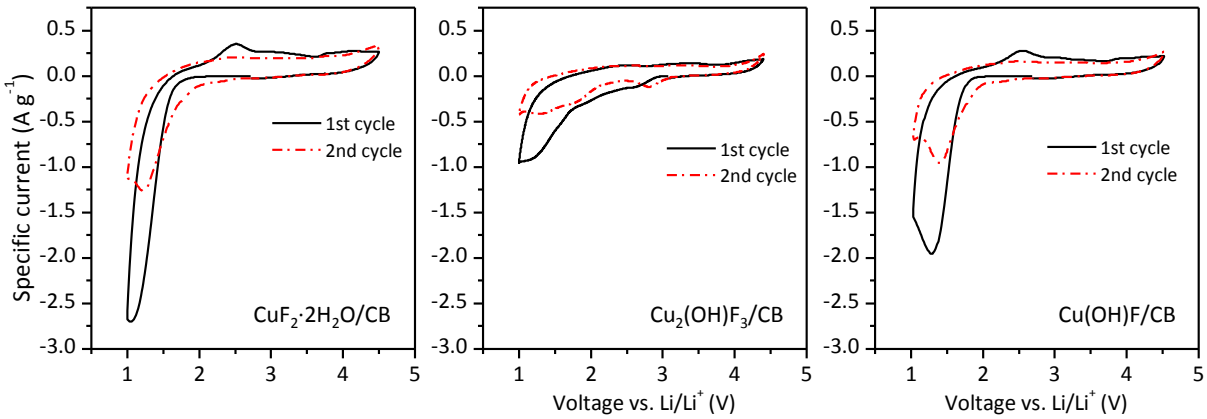

Figure 8. Cyclic voltammetry of different oxygen containing copper(II) fluoride compounds on carbon black (CB).

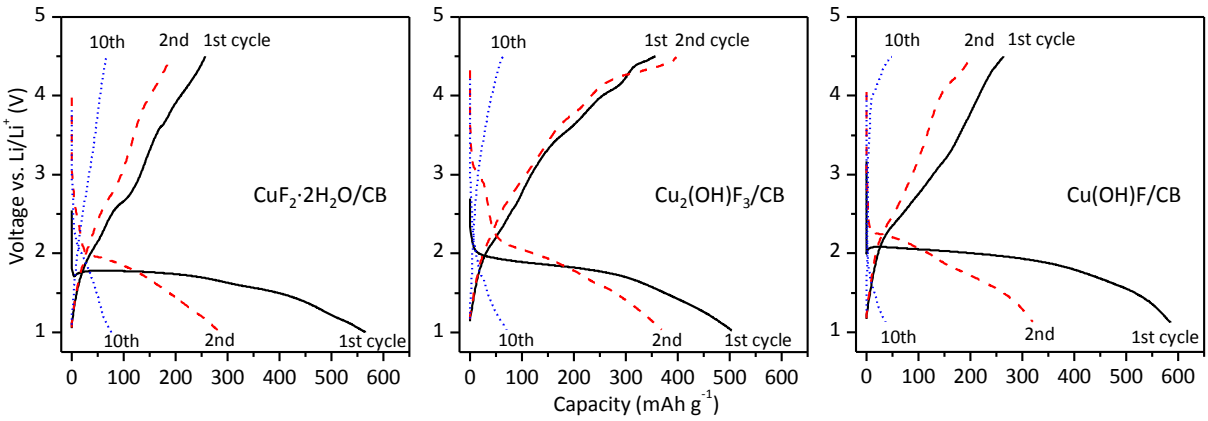

Figure 9. Galvanostatic discharge/discharge of oxygen containing copper(II) fluoride compounds on carbon black (CB) at 0.1C rate.

Figure 8 shows cyclic voltammetry and Figure 9 the galvanostatic discharge/charge profiles at different cycles of the oxygen-containing materials. Here, the potential window has been chosen to be 1-4.5 V allowing the reduction of the compounds, as it is usually done for bivalent metal fluorides.[23] The galvanostatic profiles of $CuF_2{\cdot}H_2O$, $Cu_2(OH)F_3$ and Cu(OH)F are quite similar, namely a big flat plateau of reduction located around 2 V showing higher capacity delivery compared to their theoretical capacity. The conversion occurring should be similar to that of CuF_2. This extra capacity is quite common for bivalent metal fluorides, because the operating potential of these materials is too close to the one of side reactions, which could occur between the electrolyte and the active material or the current collector. The following charge does not have specific plateau and the capacity is only partially recovered.

The subsequent discharges occur at a slightly higher potential, which could be ascribed to the decrease of ionicity of the compounds after the first discharge.[24] The three compounds show poor capacity retention (Figure 10). Charge and discharge show the same profile along all the cycles.

Accepted Manuscript

This article is protected by copyright. All rights reserved.

It is noteworthy to point out that for all of them no dissolution of metallic copper can be seen on the cyclic voltammetry and galvanostatic discharge/charge. Thus, the reduced compounds are not exactly the same as the ones formed during the discharge of pure CuF_2. Indeed, the produced insulating phase would not be pure lithium fluoride, so the metallic copper particles will not be encapsulated into an insulating phase. Furthermore, the reactions involved in the conversion occur at lower potential. Thus, it could be that the following reconversion of the materials occur at lower potential as well, avoiding reaching the potential at which the metallic copper starts dissolving into the electrolyte.

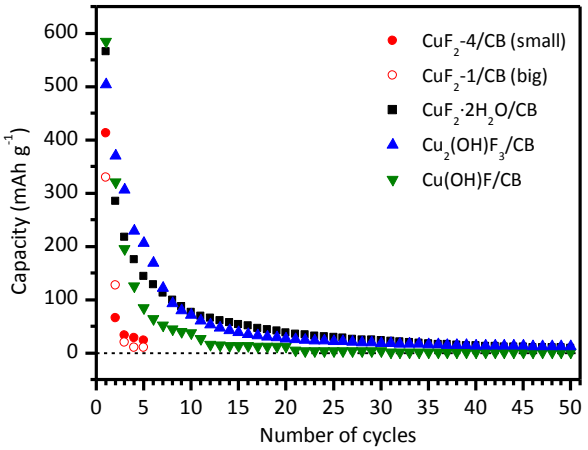

Figure 10. Capacity retention during charge/discharge cycles at 0.1C rate. CB: carbon black. CuF_2-4 ~10 nm particle size, CuF_2-1 ~100 nm particle size (cf. Table 3 and Figure 2 for details).

2.2.3 Summary of electrochemical properties

Anhydrous CuF_2 as composite with CB shows a desired high discharge capacity at a relatively high potential for cathode conversion materials. Smaller particles exhibit a higher capacity than larger particles due to the higher reactions kinetic. Unfortunately, the following charge of the compound is concealed by the dissolution of the metallic copper nanoparticles formed during the discharge. No subsequent capacity is shown arising from a reconversion of the active material, presenting therefore an irreversible behavior for CuF_2. Lithium ion half cells using our CuF_2 materials in electrode formulations show a working potential of ~2.7 V. The cell capacity depends on the particle size being 413 mAh g^{-1} for ~8 nm crystallite size and 329 mAh g^{-1} for ~12 nm crystallite size, which is ~78% and ~62% of the theoretical capacity. Correcting these values for the organic residue, and thus, referring them to pure CuF_2, the capacities are 468 mAh g^{-1} (88%) and 353 mAh g^{-1} (67%). Flat plateaus in the galvanostatic charge/discharge experiments indicate a conversion mechanism. However, the charge processes are not reversible and the capacity is nearly lost already after the 3rd charge/discharge cycle. This non-reversibility is caused by the dissolution of the metallic copper produced during the previous discharge.

If the process would be reversible the materials would be a strong competitor for replacing state of the arts compounds since the energy density delivered by the pure CuF_2 during the first discharge is twice as high as the nowadays used compounds as cathode for Li-ion batteries (~1100 Wh g^{-1} for the 10 nm sized CuF_2-4 against ~500 Wh g^{-1} for the $LiFePO_4$).

Accepted Manuscript

This article is protected by copyright. All rights reserved.

The compounds $CuF_2{\cdot}2H_2O$, $Cu_2(OH)F_3$ and Cu(OH)F as composites with carbon black also show a high capacity discharge, but at a lower working potential of ~2.0 V. This is attributed to the formation of LiOH, decreasing the free enthalpy of the conversion reaction. Compared to pure CuF_2, they show higher capacities of 500-600 mAh g^{-1}. Additionally, they show a better reversibility of the electrochemical processes. A complete loss of capacity is reached after 20-30 charge/discharge cycles. This behavior is attributed to the lithium compounds formed during reduction. Here, not pure LiF is formed, but rather a mixture of LiF and LiOH. This composite might not completely cover the formed particles of metallic Cu, ensuring still a certain electric conductivity. Furthermore, the reconversion mechanism occurs for a couple of cycles at lower potential, because the dissolution of metallic copper, which should occur at ~3.5 V, is hindered by the lower working potential of the electrode material. However, for the $CuF_2{\cdot}2H_2O$, $Cu_2(OH)F_3$ and Cu(OH)F materials the capacities along the cycles still decrease quickly, although the cyclability is slightly better than that of anhydrous CuF_2.

Although, the CuF_2 samples studied in this work show rather poor reversibility, the capacities exhibited during the first discharge, reaching up to 600 mAh g^{-1}, make them interesting cathode materials for primary battery applications.

3 Conclusion

Nanoscale CuF_2 can be successfully prepared from copper(II) alkoxides and HF, using either solvothermal synthesis in THF or liquid anhydrous HF under strict exclusion of moisture. Depending on the reaction conditions, nanoparticles of a size between 10 and 100 nm are formed. We show here the possibility to implement a new synthesis approach allowing the nanosizing of CuF_2. This is a far more suitable way for any applications in electrochemistry than the ball milling of micron-sized particles, which is commonly performed in order to study intrinsically low conductive compounds.

CuF_2 is a very hygroscopic compound, readily forming hydrates and hydroxide fluorides upon contact with moisture. Out of these, only Cu(OH)F is stable under air. Novel synthesis routes were developed to obtain the phase pure compounds $CuF_2{\cdot}2H_2O$ and $Cu_2(OH)F_3$. Both of them are unstable under air and undergo hydrolysis.

Based on the comprehensive synthesis routes developed in this work (cf. Figure 5), we have investigated the electrochemical properties of copper(II) fluoride and derivatives in an attempt to evaluate their applicability in Li-Ion batteries and to assess a clear structure-property correlation. All in all, it can be stated that although the theoretical capacity and potential of copper(II) fluoride make it a potential candidate, its high potential vs. Li/Li^+ leads to the dissolution of metallic copper during the charge and to irreversible operation. On the other hand, hydroxyfluorides and hydrated copper fluorides show a partial reversibility, but also, as expected, a lower working potential making them not as interesting as pure metal fluorides.

Accepted Manuscript

This article is protected by copyright. All rights reserved.

4 Experimental Part

4.1 Reactants

Methanol was obtained from Sigma Aldrich Co. (99.6%) and refluxed over Mg for 3 days. Other alcohols (ethanol, *n*-propanol, *n*-butanol, *t*-butanol) were refluxed over Na for 3 days.

Tert-butyl acetate was dried by stirring over freshly dehydrated molecular sieve 4 Å for 3 days. Tetrahydrofuran was refluxed over sodium wire for 3 days.

Copper(II) chloride $CuCl_2$ was obtained from ABCR, lithium methoxide was obtained from Strem. These compounds were handled and stored under argon in a glove box.

Solutions of anhydrous HF in methanol, ethanol and tetrahydrofuran were prepared by bubbling a gaseous HF/argon mixture through the solvent in a FEP bottle under cooling. The exact procedure is described elsewhere.[25] *Caution: HF is a hazardous agent and has to be used under restricted conditions only!*

4.2 Synthesis of copper precursors

As long as not stated otherwise, all work was carried out under argon using standard Schlenk technique and the products are stored under argon atmosphere. *Caution: HF is a hazardous agent and has to be used under restricted conditions only!*

Abbreviations: PFA = perfluoroalkoxy polymer, THF = tetrahydrofuran, Me = CH_3, *t*Bu = *tert*-C_4H_9.

$Cu(OMe)_2$.[26] 10.86 g (80.8 mmol) brown $CuCl_2$ was dissolved in 100 ml methanol resulting in a clear green solution. 6.14 g LiOMe (161.6 mmol) was dissolved in 80 ml methanol. The Li solution was transferred into the Cu solution under vigorous stirring; the vessel was purged with 20 ml methanol. A mixture of blue and green precipitates is obtained, which are $Cu(OMe)_2$ and Cu(OMe)Cl, respectively. The reaction mixture is refluxed for 2-3 hours. The green precipitate now vanished. After cooling and sedimentation overnight, the blue precipitate is filtered and washed repeatedly with methanol (ca. 7-10 times with portions of 60 ml), until the filtrate contains no more chloride (tested with $AgNO_3$). The blue residue was dried in vacuum at 40°C. Yield: 9.70 g $Cu(OMe)_2$ (77.2 mmol, =95.5%).

$Cu(O$*t*$Bu)_2$.[26] 5.05 g (40.2 mmol) blue $Cu(OMe)_2$ was dispersed in 80 ml *tert*-butyl acetate CH_3COO-*t*Bu and refluxed for 1 h. The solid color turned from deep blue to slightly greenish blue. After this, the reaction mixture is evaporated in vacuum to $^1/_4$ of its original volume to remove formed methyl acetate. The procedure was repeated after adding another 50 ml of *tert*-butyl acetate. After final cooling, remaining solvent was filtered off, and the residue was dried in vacuum at 40°C. Yield: 4.22 g $Cu(O$*t*$Bu)_2$ (20.1 mmol, =50%).

$CuF_2 \cdot 2H_2O$. 15,12 g $CuCO_3 \cdot Cu(OH)_2$ (68.4 mmol) was suspended in 30 ml ethanol in an open PFA flask. 15.1 ml of 27.16 M ethanolic HF (410.4 mmol, i.e. Cu:HF = 1:3) was added and stirred for 1 hour, until no CO_2 evolves anymore. The light blue precipitate is filtered and dried at 50°C in vacuum. Yield: 17.55 g (172.6 mmol, =93.3%). Elemental analysis calcd (%): Cu 46.2, F 27.6; found batch 1/2: 46.3/46.8, 24.4/27.2. XRD $CuF_2 \cdot 2H_2O$ (PDF 6-143).

$Cu_2(OH)F_3$. 1.00 g $CuF_2 \cdot 2H_2O$ (7.27 mmol) was packed three times crosswise into aluminum foil to ensure a self-generated atmosphere during decomposition. This pack was annealed in a muffle type furnace for 3 h at 160°C at the open air. The still hot pack is transferred into an

Accepted Manuscript

This article is protected by copyright. All rights reserved.

argon filled Schlenk tube. After cooling under argon, the tube was transferred into an argon filled glove box, and the foil pack was opened. A pale blue powder is obtained. Yield: 0.691 g (3.44 mmol, =94.6%). Elemental analysis calcd (%): Cu 63.2, F 28.1; found 60.6, 28.3. XRD $Cu_2(OH)F_3$ (PDF 6-170).

Cu(OH)F.[16] 5.00 g $CuF_2{\cdot}2H_2O$ (36.3 mmol) was suspended in 100 ml water in an open PFA flask. The flask was heated in an oil bath at the open air to boiling for 5 h. Formed HF was allowed to evaporate. Evaporated water was successively replaced. Meanwhile a light blue precipitate was formed. After cooling, the precipitate was filtered off, followed by drying at 80°C. Yield: 2.33 g (23.4 mmol, =64.5%). The product is stable at air, but decomposes into CuO in contact with cold water within one day. Analysis (theoretical values in brackets): Elemental analysis calcd (%): Cu 63.8, 19.1; found: 63.8, 19.1. XRD Cu(OH)F (PDF 7-306).

4.3 Synthesis of *nano*-CuF_2

All reactions were carried out under inert argon atmosphere. Products were stored under argon. *Caution: HF is a hazardous agent and has to be used under restricted conditions only!*

CuF_2 – solvothermal reaction. *General procedure*: In an autoclave with Teflon inset (total volume 40 ml) 2.00 g $Cu(OMe)_2$ or 3.34 g $Cu(O\mathit{t}Bu)_2$ (15.92 mmol) were filled in. 10.0 ml of 17.59 M HF solution in THF (176 mmol, i.e. Cu:F ≈ 1:11) were added. The vessel was closed, and then annealed for 2.5 h at 150°C. The pressure in the autoclave raises to approximately 8 bar. After cooling, the autoclave was opened, and the content was transferred into a PFA flask. The reaction mixture consisted of a white precipitate in a light brown supernatant liquid. The brown color was less distinct for the $Cu(O\mathit{t}Bu)_2$ precursor. By cooling the flask to -20°C, more precipitate is formed. The precipitate was then filtered off. The residue was washed with small amounts of pre-cooled (-20°C) THF and dried in vacuum at room temperature. Depending on the number of washing cycles, a white to slightly brownish product was obtained. The yields vary from 0.5 to 0.7 g. The product still contains absorbed organic residue (ca. 6-8%), i.e. the total yield of CuF_2 is between 28 and 40%. Subsequent washing with THF reduces the yield. Obviously, CuF_2 is slightly soluble in THF.

CuF_2 – liquid HF. 2.00 g $Cu(OMe)_2$ or 3.34 g $Cu(O\mathit{t}Bu)_2$ (15.92 mmol) were placed in a 250 ml three necked PFA flask, equipped with a magnetic stirrer. The flask was cooled to -70°C and hold at this temperature. A gas stream of HF/argon (ratio ca. 1:1) was introduced, until ca. 10 ml of liquid HF were formed. Meanwhile the solid changed color from blue to white, but did not dissolve. The reaction mixture was stirred for 10 min at -70°C. Then the cooling was removed and the mixture was stirred under a light argon flow, until HF was evaporated. Residual HF was removed in vacuum. The yield is usually around 1.4 g. The product still contains absorbed organic residue (ca. 10-12%), i.e. the total yield of CuF_2 is around 75-80%.

For detailed analysis data cf. Table 3.

4.4 Characterization

XRD. X-ray diffraction were measured on a Seiffert 3003TT diffractometer (Bragg-Brentano geometry) using Cu K_α radiation (if not stated otherwise). Samples were prepared under argon in the glove box. For the measurement they were protected with amorphous polystyrene foil and sealed with Kel-F grease. The average crystallite size L was calculated

Accepted Manuscript

This article is protected by copyright. All rights reserved.

from Scherrer's equation $L \approx \lambda/(\beta_{khl}\cos\theta)$. The measured linewidth $\beta_{m,hkl}(2\theta)$ was corrected with the intrinsic linewidth $\beta_0 = 0.12°$ of the equipment: $\beta_{hkl} = \sqrt{\beta_{m,hkl}^2 - \beta_0^2}$.

FTIR. Spectra were obtained using a Varian 3000 spectrometer in ATR mode (golden gate, diamond crystal). The design of the ATR cell allowed handling and measuring of substances in an argon atmosphere under exclusion of moisture.

TEM. Transmission electron microscopy images were recorded on a Philips CM 200 microscope equipped with a LaB_6 cathode and operated at 200 kV.

Elemental analysis. Cu content was determined by dissolving the compound in diluted hydrochloric acid and titration with 0.01 M $Na_2S_2O_3$ using amylose as indicator. F content was determined by soda-potash fusion followed by measuring the total fluoride concentration with a fluoride sensitive electrode. CHNS analysis was done using a standard EuroVector EuroEA 3000 analyzer.

4.5 Electrochemical testing

All the subsequent operations were realized in an Ar-filled glove box.

Materials preparation. The active materials were beforehand mixed together with appropriate amounts (see below) of Carbon Black (Timcal, super C) by the mean of a planetary mill PULVERISETTE 7) for 8 h at 750 rpm using zirconia beakers and beads under argon atmosphere. 0.5 g of the mixed powder was used for each ball milling, the ratio of this powder to the zirconia beads was 1:14.

Electrodes preparation. The collected milled powders were blended with poly(vinyliden-difluoride) (PVdF, Alfa Aesar) in N-Methylpyrrolidone (NMP, Sigma Aldrich , anhydrous 99.5%). The final mass ratio between the active materials, carbon black and PVdF was 65:25:10. The homogeneous slurries were spread over aluminum foils with a razor blade for a thickness of 20 µm and left more than two days to allow the NMP to be evaporated. Then disks of 18 mm of diameter were cut to be used as electrodes. The electrochemical performances were evaluated via half-cell tests using 1 M $LiPF_6$ (ABCR, 99.9% battery grade) in a non-aqueous mixture of ethylene carbonate (EC, ABCR, 99%), propylene carbonate (PC, ABCR, 99%) and dimethyl carbonate (DMC, ABCR, 99%) with a volume ratio of 1:1:1 as an electrolyte, and glass fiber separator (Whatman) against metallic lithium disks (Sigma) on a Bio-Logic VMP3 potentiostat/galvanostat. The calculations of the specific capacities are done taking in account only the active materials, including the organic residue, but excluding the carbon black added during the ink formulation and ball milling process. The uncertainties related to the calculations of the capacities given in the manuscript based on at least two batteries run in parallel were always below 4%.

5 Acknowledgements

Dr. F. Emmerling (BAM) is gratefully acknowledged for measuring X-ray diffraction data of Cu(OR)F. Dr. M. Feist (HU Berlin) is gratefully acknowledged for measuring thermal analysis of $CuF_2{\cdot}2H_2O$. Florian Schütz is gratefully acknowledged for assistance in working with liquid HF. This work was partially funded by the Deutsche Forschungsgemeinschaft DFG KE 489/21-1.

Accepted Manuscript

This article is protected by copyright. All rights reserved.

6 References

[1] a) J. Cabana, L. Monconduit, D. Larcher, M. R. Palacín, *Adv. Mater.* **2010**, *22*, E170-E192; b) N. Nitta, F. Wu, J. T. Lee, G. Yushin, *Mater. Today* **2015**, *18*, 252-264.

[2] J. K. Seo, H.-M. Cho, K. Takahara, K. W. Chapman, O. J. Borkiewicz, M. Sina, Y. S. Meng, *Nano Research* **2017**.

[3] a) F. Wang, R. Robert, N. A. Chernova, N. Pereira, F. Omenya, F. Badway, X. Hua, M. Ruotolo, R. Zhang, L. Wu, V. Volkov, D. Su, B. Key, M. S. Whittingham, C. P. Grey, G. G. Amatucci, Y. Zhu, J. Graetz, *J. Am. Chem. Soc.* **2011**, *133*, 18828-18836; b) X. Hua, R. Robert, L.-S. Du, K. M. Wiaderek, M. Leskes, K. W. Chapman, P. J. Chupas, C. P. Grey, *J. Phys. Chem. C* **2014**, *118*, 15169-15184.

[4] a) L. D. Carlo, D. E. Conte, E. Kemnitz, N. Pinna, *Chem. Commun.* **2014**, *50*, 460-462; b) F. Badway, A. N. Mansour, N. Pereira, J. F. Al-Sharab, F. Cosandey, I. Plitz, G. G. Amatucci, *Chem. Mater.* **2007**, *19*, 4129-4141.

[5] a) J. Chun, C. Jo, S. Sahgong, M. G. Kim, E. Lim, D. H. Kim, J. Hwang, E. Kang, K. A. Ryu, Y. S. Jung, Y. Kim, J. Lee, *ACS App. Mater. Interfaces* **2016**, *8*, 35180-35190; b) X. Wang, W. Gu, J. T. Lee, N. Nitta, J. Benson, A. Magasinski, M. W. Schauer, G. Yushin, *Small* **2015**, *11*, 5164-5173.

[6] C. M. Wheeler, H. M. Haendler, *J. Am. Chem. Soc.* **1954**, *76*, 263-264.

[7] a) C. Billy, H. M. Haendler, *J. Am. Chem. Soc.* **1957**, *79*, 1049-1051; b) P. Fischer, W. Hälg, D. Schwarzenbach, H. Gamsjäger, *J. Phys. Chem. Solids* **1974**, *35*, 1683-1689; c) J. C. Taylor, P. W. Wilson, *J. Less Common Met.* **1974**, *34*, 257-259.

[8] a) F. Ebert, H. Woitinek, *Z. Anorg. Allg. Chem.* **1933**, *210*, 269-272; b) O. Ruff, M. Giese, *Z. Anorg. Allg. Chem.* **1934**, *219*, 143-148.

[9] H. von Wartenberg, *Z. Anorg. Allg. Chem.* **1939**, *241*, 381-394.

[10] a) R. Juza, H. Hahn, *Z. Anorg. Allg. Chem.* **1939**, *241*, 172-178; b) W. J. de Haas, B. H. Schultz, J. Koolhaas, *Physica* **1940**, *7*, 57-69; c) H. M. Haendler, F. A. Johnson, D. S. Crocket, *J. Am. Chem. Soc.* **1958**, *80*, 2662-2664; d) K. C. Patil, E. A. Secco, *Can. J. Chem.* **1972**, *50*, 1529-1530; e) S. I. Troyanov, I. Morozov, Y. M. Korenev, *Russ. J. Inorg. Chem.* **1993**, *38*, 909-989.

[11] T. Y. Glazunova, A. I. Boltalin, P. P. Fedorov, *Russ. J. Inorg. Chem.* **2006**, *51*, 983-987.

[12] M. Mosiadz, K. L. Juda, S. C. Hopkins, J. Soloducho, B. A. Glowacki, *J. Fluorine Chem.* **2012**, *135*, 59-67.

[13] E. Kemnitz, J. Noack, *Dalton Trans.* **2015**, *44*, 19411-19431.

[14] a) D. D. Wagman, W. H. Evans, V. B. Parker, R. H. Schumm, I. Halow, S. M. Bailey, K. L. Churney, R. L. Nuttall, *J. Phys. Chem. Ref. Data* **1982**, *11*, Suppl. 2; b) M. Binnewies, E. Milke, *Thermochemical Data of Elements and Compounds*, Wiley-VCH, Germany, Weinheim, **1999**.

[15] P. Ramamurthy, E. A. Secco, *Can. J. Chem.* **1969**, *47*, 2185-2190.

[16] J. J. Berzelius, *Annalen der Physik* **1824**, *77*, 169-230.

[17] L. Li, R. Jacobs, P. Gao, L. Gan, F. Wang, D. Morgan, S. Jin, *J. Am. Chem. Soc.* **2016**, *138*, 2838-2848.

[18] Q. Guan, J. Cheng, X. Li, W. Ni, B. Wang, *Chin. J. Chem .* **2017**, *35*, 48-54.

[19] S. Geller, W. L. Bond, *J. Chem. Phys.* **1958**, *29*, 925-930.

[20] G. Giester, E. Libowitzky, *Z. Kristallogr.* **2003**, *218*, 351.

Accepted Manuscript

This article is protected by copyright. All rights reserved.

[21] H. R. Oswald, A. Reller, H. W. Schmalle, E. Dubler, *Acta Crystallographica Section C* **1990**, *46*, 2279-2284.

[22] D. E. Conte, L. Di Carlo, M. T. Sougrati, B. Fraisse, L. Stievano, N. Pinna, *J. Phys. Chem. C* **2016**, *120*, 23933-23943.

[23] Y. T. Teng, F. Wei, R. Yazami, *J. Alloys Compd.* **2015**, *653*, 434-443.

[24] Y. T. Teng, S. S. Pramana, J. Ding, T. Wu, R. Yazami, *Electrochim. Acta* **2013**, *107*, 301-312.

[25] T. Krahl, D. Broßke, K. Scheurell, B. Lintner, E. Kemnitz, *J. Mater. Chem. C* **2016**, *4*, 1454-1466.

[26] J. V. Singh, B. P. Baranwal, R. C. Mehrotra, *Z. Anorg. Allg. Chem.* **1981**, *477*, 235-240.

Accepted Manuscript

This article is protected by copyright. All rights reserved.

10.1002/chem.201800207

TOC Graphics

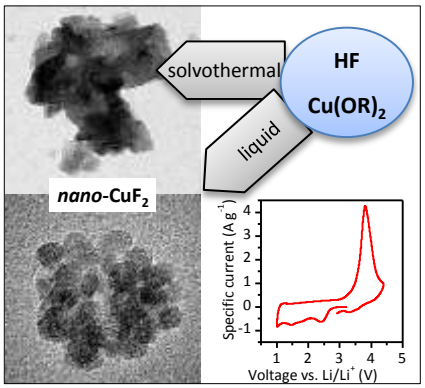

TOC Text

Nanoscale CuF_2 is directly prepared by reaction of anhydrous HF with $Cu(OR)_2$ without a further milling process.

It has a high electrochemical potential of 2.7 V in lithium ion batteries. Smaller particles show higher capacities than larger particles, but the capacity is lost after recharge. Hydroxylated CuF_2 has a lower potential but a higher capacity and a slightly better cyclability.

Accepted Manuscript

This article is protected by copyright. All rights reserved.